EUROPEAN JOURNAL OF PURE AND APPLIED MATHEMATICS
2025, Vol. 18, Issue 1, Article Number 5843
ISSN 1307-5543 – ejpam.com
Published by New York Business Global

An Efficient Adaptive Time-stepping Method for the Modeling of Epidemic Dynamics

Junseok Kim

Department of Mathematics, Korea University, Seoul 02841, Republic of Korea

Abstract. In this study, we present a novel and efficient adaptive time-stepping method for modeling epidemic dynamics. Examples of mathematical epidemic models include the susceptible-infected-recovered (SIR) model, the susceptible-exposed-infected-recovered (SEIR) model, the susceptible -infected-susceptible (SIS) model, the susceptible-infected-recovered-susceptible (SIRS) model, and the susceptible-infected-quarantined-recovered (SIQR) model. More complex models include the maternal immunity susceptible-infected-recovered (MSIR) model, the age-structured SEIR model, and stochastic epidemic models. These models are designed to capture specific disease characteristics, such as latency, immunity duration, and intervention impacts, and are essential tools for studying the dynamics of infectious diseases in diverse populations. The proposed adaptive time-stepping method is based on the total magnitude of the summation of compartment population differences after a single time step. Unlike other adaptive methodologies, the proposed algorithm does not require recalculations to satisfy a given tolerance and achieves the desired accuracy with a single update. Therefore, the adaptive time-stepping method is both straightforward and efficient. Several numerical tests are conducted to demonstrate the superior performance of the proposed method.

2020 Mathematics Subject Classifications: 65L05, 65L06, 92D30

Key Words and Phrases: adaptive time-stepping, epidemic mathematical model, numerical method, SIR model

1. Introduction

It is indisputable that mathematical epidemic models hold paramount importance in the formulation of strategies in order to prevent the transmission of infectious diseases, including COVID-19, because they provide quantitative insights into transmission patterns and inform evidence-based policymaking [14]. These mathematical epidemic models provide essential tools for the estimation of important epidemiological parameters, such as the basic reproduction number, and enable researchers to assess diverse intervention measures [2]. This approach enables public health authorities to implement timely and effective responses. Such measures reduce the impact of large-scale outbreaks

DOI: https://doi.org/10.29020/nybg.ejpam.v18i1.5843

Email address: cfdkim@korea.ac.kr (J. Kim)

[15]. Therefore, epidemic models are indispensable in epidemiology and public health research because they expedite a systematic examination of disease transmission and control strategies. Mathematical frameworks such as the susceptible-infected-recovered (SIR) [18], susceptible-exposed-infected-recovered (SEIR) [10], susceptible-infected-susceptible (SIS) [17], susceptible-infected-recovered-susceptible (SIRS) [11], susceptible-infected - quarantined-recovered (SIQR) [13], maternal immunity susceptible-infected -recovered (MSIR) [16], age-structured SEIR [4], and stochastic variants [12] frequently appear in studies that resolve diverse aspects of infectious diseases. Each framework isolates essential characteristics, such as latency periods, immunity duration, or the impact of interventions. These characteristics are crucial for the design of effective prevention and mitigation strategies.

A wide range of computational methods exists for the simulation of epidemic models. Among these approaches, robust numerical methods offer accurate and reliable predictions. However, many standard methods rely on fixed time steps that do not adapt to significant changes in a system's dynamics. This shortcoming can produce unnecessary computational overhead or diminished accuracy when the model enters regions of greater complexity or rapid change. Consequently, there is a growing need for computational methods that can automatically adjust time steps while maintaining efficiency.

Adaptive time-stepping approaches resolve this need by modifying the step size in response to variations in the underlying model equations [9]. This flexibility reduces redundant calculations and preserves the accuracy of the results. However, many existing adaptive schemes require repeated recalculations to enforce a prescribed tolerance, which diminishes their overall efficiency. This paper introduces a novel adaptive time-step selection method for epidemic models that uses the total magnitude of the summation of compartment population differences after a single step as the sole criterion for time-step adjustment. This approach achieves the required accuracy with a single update and eliminates additional recalculations to satisfy tolerance requirements. Furthermore, the criterion for adaptive time-stepping is more intuitive compared to previous criteria based on error estimation. The proposed method is straightforward to implement and compatible with the aforementioned broad range of epidemic models. Numerical experiments confirm the method's efficiency.

The organization of this article is described as follows. Section 2 presents the proposed adaptive time-stepping method. Section 3 provides computational tests to validate the efficiency and accuracy of the proposed method. Section 4 concludes the article with a discussion of the main findings and potential future work. Additionally, the Appendix includes the MATLAB source code for the proposed method, which can be used as a computational tool for further analysis and replication of results.

2. Proposed Computational Method

The standard SIR model is considered to demonstrate the proposed adaptive time-stepping algorithm for mathematical epidemic models [1]. The SIR model describes the transmission of infectious diseases by dividing the population into three groups: susceptible

(S), representing individuals at risk of infection; infected (I), representing those currently infected and capable of transmitting the disease; and recovered (R), representing individuals who have recovered and gained immunity. The standard SIR model is formulated as follows:

$$\frac{dS(t)}{dt} = -\beta S(t)I(t), \tag{1}$$
$$\frac{dI(t)}{dt} = \beta S(t)I(t) - \gamma I(t), \tag{2}$$
$$\frac{dR(t)}{dt} = \gamma I(t). \tag{3}$$

Here, $S(t)$, $I(t)$, and $R(t)$ represent the numbers of susceptible, infected, and recovered individuals at time t, corresponding to those not currently infected, those actively infected, and those who have recovered, respectively. The parameter β is the average number of random contacts an individual has per unit time, while $1/\gamma$ denotes the average duration for an infected individual to recover [3]. To effectively solve the governing equations of the SIR model (1)–(3) and capture the dynamics of disease transmission, we propose a novel numerical method that uses an adaptive time-stepping approach designed to the nonuniform temporal changes in the model. Let $S_n = S(t_n)$, $I_n = I(t_n)$, and $R_n = R(t_n)$ for $n = 1, \ldots,$ where $t^n = t^{n-1} + \Delta t^n$, for $n \geq 1$, Δt^n is the variable time step size, and $t^0 = 0$. The SIR model (1)–(3) can be discretized using a finite difference method [8] as follows:

$$\frac{S_{n+1} - S_n}{\Delta t^{n+1}} = -\beta S_n I_n, \tag{4}$$
$$\frac{I_{n+1} - I_n}{\Delta t^{n+1}} = \beta S_n I_n - \gamma I_n, \tag{5}$$
$$\frac{R_{n+1} - R_n}{\Delta t^{n+1}} = \gamma I_n, \tag{6}$$

which can be rewritten as follows:

$$S_{n+1} = S_n - \Delta t^{n+1}\beta S_n I_n, \tag{7}$$
$$I_{n+1} = I_n + \Delta t^{n+1}(\beta S_n I_n - \gamma I_n), \tag{8}$$
$$R_{n+1} = R_n + \Delta t^{n+1}\gamma I_n. \tag{9}$$

Using a recently developed methodology [6], we describe an adaptive time-stepping algorithm for epidemic mathematical models. We define a tolerance *tol* to set the maximum allowable displacement of the computational solution during a time step. By multiplying both sides of Eqs. (4)–(6) by Δt^{n+1}, the following equations are derived.

$$S_{n+1} - S_n = -\Delta t^{n+1}\beta S_n I_n, \tag{10}$$
$$I_{n+1} - I_n = \Delta t^{n+1}(\beta S_n I_n - \gamma I_n), \tag{11}$$
$$R_{n+1} - R_n = \Delta t^{n+1}\gamma I_n. \tag{12}$$

Let *evol* be the total magnitude of the summation of each compartment's population differences after a single time step:

$$\begin{aligned} evol &= |S_{n+1} - S_n| + |I_{n+1} - I_n| + |R_{n+1} - R_n| \\ &= \Delta t^{n+1}\beta S_n I_n + |\Delta t^{n+1}(\beta S_n I_n - \gamma I_n)| + \Delta t^{n+1}\gamma I_n \\ &= \Delta t^{n+1}(\beta S_n I_n + |\beta S_n I_n - \gamma I_n| + \gamma I_n). \end{aligned} \tag{13}$$

In this study, it is important to note that we use Eq. (13) for *evol*, which indicates that our objective is to control the evolution by accounting for population differences among the considered groups. We may use other criterion such as

$$evol = \sqrt{(S_{n+1} - S_n)^2 + (I_{n+1} - I_n)^2 + (R_{n+1} - R_n)^2}. \tag{14}$$

Let us define *tol* as a given tolerance. We require that Δt^{n+1} satisfy the following condition: $evol \leq tol$, that is,

$$\Delta t^{n+1}(\beta S_n I_n + |\beta S_n I_n - \gamma I_n| + \gamma I_n) \leq tol. \tag{15}$$

From Eq. (15), we obtain the following constraint on the time step sizes:

$$\Delta t^{n+1} \leq \frac{tol}{\beta S_n I_n + |\beta S_n I_n - \gamma I_n| + \gamma I_n}. \tag{16}$$

This constraint ensures that the time step is adjusted appropriately to satisfy the tolerance requirement *tol*. Then, we use

$$\Delta t^{n+1} = \min\left(\frac{tol}{\beta S_n I_n + |\beta S_n I_n - \gamma I_n| + \gamma I_n},\ \Delta t_{\max}\right). \tag{17}$$

Here, the maximum time step size, $\Delta t_{\max}$, is predetermined to guarantee stability. Hence, the numerical solutions at each time step are provided in Eqs. (10)–(12). This process is repeated while satisfying the condition $t^n + \Delta t^{n+1} \leq T$ to compute the numerical solutions of $S(T)$, $I(T)$, and $R(T)$. When selecting adaptive time steps, it is possible for t^{n+1} to exceed the specified final time T. To prevent this, if $t^{n+1} = t^n + \Delta t^{n+1} > T$, the time step t^{n+1} is adjusted to $T - t^n$.

3. Computational Experiments

This section presents a series of computational experiments designed to thoroughly evaluate the effectiveness, accuracy, and high performance of the proposed method across different scenarios, which highlights its robustness and practical applicability in solving epidemic problems with improved computational efficiency and reliability.

3.1. Effect of the tolerance, *tol*

Figure 1(a) shows the temporal evolution of the susceptible $S(t)$, infected $I(t)$, and recovered $R(t)$ populations, along with the adaptive time-stepping behavior in the discrete time grid. The parameters are $\beta = 0.3$, $\gamma = 0.1$, and initial conditions $S_0 = 0.99$, $I_0 = 0.01$, and $R_0 = 0$. $S(t)$ decreases over time and represents the decline of the susceptible population due to infection. $I(t)$ initially increases, reaching a peak, and then declines as individuals recover. $R(t)$ increases steadily, showing the accumulation of recovered individuals. Figure 1(b) shows the adaptive time step size (Δt^{n+1}) and the corresponding time grid (t^{n+1}). The time step size adjusts dynamically, decreasing during rapid changes (e.g., the peak of $I(t)$) and increasing as the system approaches a steady state. The adaptive method ensures both accuracy and computational efficiency. In this computation, a tolerance of tol = 0.1 and a maximum step size of $\Delta t_{\max} = 3$ are used.

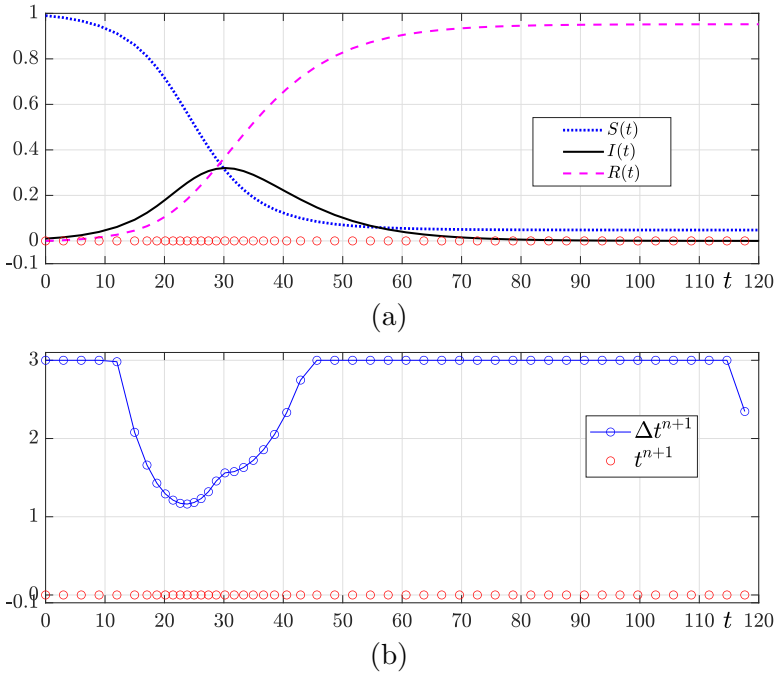

Figure 1: (a) Computational results for $S(t)$, $I(t)$, and $R(t)$ with an adaptive discrete time grid (red circles). (b) The adaptive discrete time grid and corresponding time steps. The parameters used are $\beta = 0.3$, $\gamma = 0.1$, $S_0 = 0.99$, $I_0 = 0.01$, $R_0 = 0$, $T = 120$, $tol = 0.1$, and $\Delta t_{\max} = 3$.

When the tolerance is reduced to tol = 0.01, the adaptive time step size Δt^{n+1} decreases further during rapid transitions in the system (e.g., around the peak of $I(t)$) to maintain higher accuracy as shown in Fig. 2(a). As a result, more time steps are required to accurately capture the dynamics of the system. As the system approaches a steady state, the step size increases, which optimizes computational efficiency and maintains accuracy. The adaptive method ensures reliable numerical results for all populations. However, compared to the case with tol = 0.1, the computation demands higher precision and involves more steps to satisfy the stricter tolerance requirement as shown in Fig. 2(b).

For this computation, the maximum step size of $\Delta t_{\max} = 3$ is used.

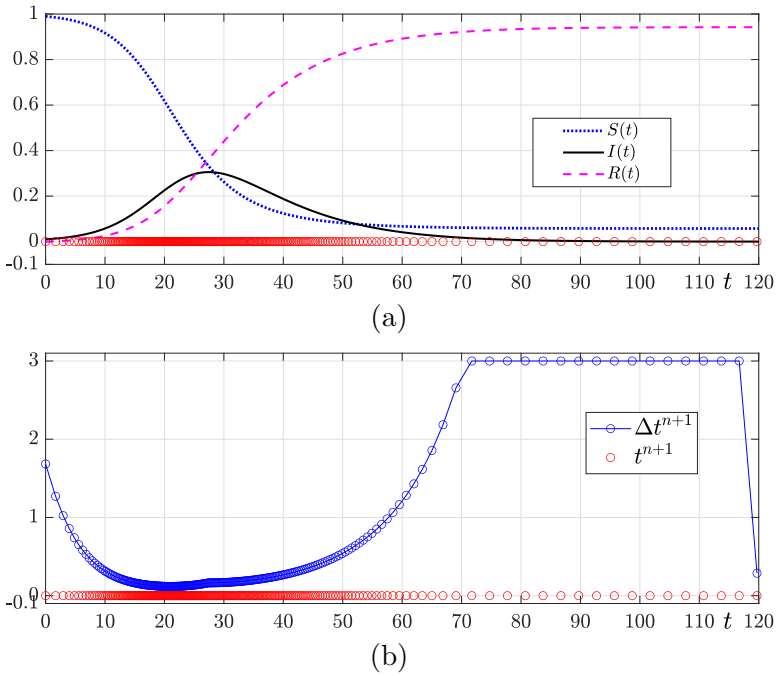

Figure 2: (a) Computational results for $S(t)$, $I(t)$, and $R(t)$ with an adaptive discrete time grid (red circles). (b) The adaptive discrete time grid and corresponding time steps. The parameters used are $\beta = 0.3$, $\gamma = 0.1$, $S_0 = 0.99$, $I_0 = 0.01$, $R_0 = 0$, $T = 120$, $tol = 0.01$, and $\Delta t_{\max} = 3$.

Figure 3 illustrates the temporal evolution of the susceptible $S(t)$, infected $I(t)$, and recovered $R(t)$ populations, alongside the adaptive time-stepping behavior for a discrete time grid. The parameters used are $\beta = 0.3$, $\gamma = 0.1$, $S_0 = 0.99$, $I_0 = 0.01$, $R_0 = 0$, with a total simulation time of $T = 120$, a tolerance of tol $= 0.001$, and a maximum step size of $\Delta t_{\max} = 3$. Figure 3(a) shows the evolution of the populations. $S(t)$ decreases over time due to infection, $I(t)$ initially rises to a peak before declining as individuals recover, and $R(t)$ steadily increases, representing the cumulative number of recovered individuals. Figure 3(b) presents the adaptive time step size Δt^{n+1} and the corresponding time points t^{n+1}. Compared to results with larger tolerances, the smaller tol $= 0.001$ results in significantly smaller time steps during periods of rapid change, such as the peak of $I(t)$. As the system approaches a steady state, the step size increases and ensures computational efficiency while maintaining accuracy. This stricter tolerance results in finer resolution and more accurate modeling of the system dynamics, especially during critical transitions. In this test, using a fully explicit Euler method results in a CPU time that is double that of the adaptive algorithm.

The value of *tol* is selected based on the specific needs and objectives of the user and is carefully determined according to the scale and characteristics of the problem under consideration. This ensures that the chosen tolerance value aligns with the desired level of accuracy and the nature of the computational model being analyzed.

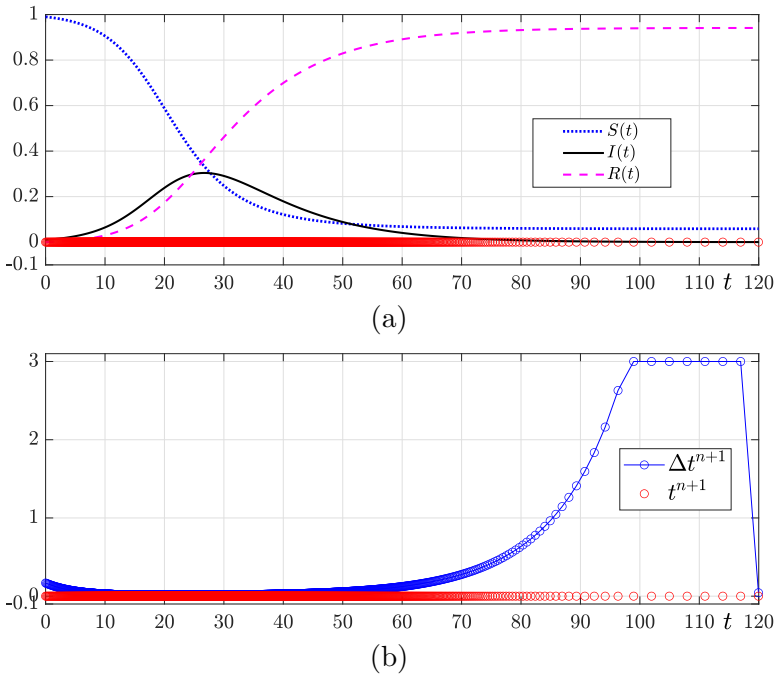

Figure 3: (a) Computational results for $S(t)$, $I(t)$, and $R(t)$ with an adaptive discrete time grid (red circles). (b) The adaptive discrete time grid and corresponding time steps. The parameters used are $\beta = 0.3$, $\gamma = 0.1$, $S_0 = 0.99$, $I_0 = 0.01$, $R_0 = 0$, $T = 120$, $tol = 0.001$, and $\Delta t_{\max} = 3$.

3.2. Effect of the maximum step size, $\Delta t_{\max}$

Next, we investigate the effect of the maximum step size, $\Delta t_{\max}$. The parameters are set as $\beta = 0.3$, $\gamma = 0.1$, tol $= 0.1$, with initial conditions $S_0 = 0.99$, $I_0 = 0.01$, and $R_0 = 0$. The computations are conducted for three different values of the maximum step size of $\Delta t_{\max}$. Figure 4(a) presents the computational results for $S(t)$, $I(t)$, and $R(t)$ under three different values of the maximum step size, $\Delta t_{\max}$. Figure 4(b) illustrates the adaptive discrete time steps corresponding to these three values of the maximum step size. From these results, it can be observed that the numerical solution becomes less accurate when an excessively large $\Delta t_{\max}$ is used. This is because, during the initial stages when the solution is smooth, larger time steps are used, which leads to significant errors. Consequently, using an excessively large maximum time step is not advisable.

4. Conclusions

In this study, we proposed an efficient adaptive time-stepping method for modeling epidemic dynamics. By dynamically adjusting the time step size based on the magnitude of changes in population compartments, the method achieved both high accuracy and computational efficiency. Numerical experiments demonstrated the effectiveness of the proposed approach in capturing the dynamics of susceptible, infected, and recovered populations under various tolerance levels. The results confirmed that the adaptive method provides

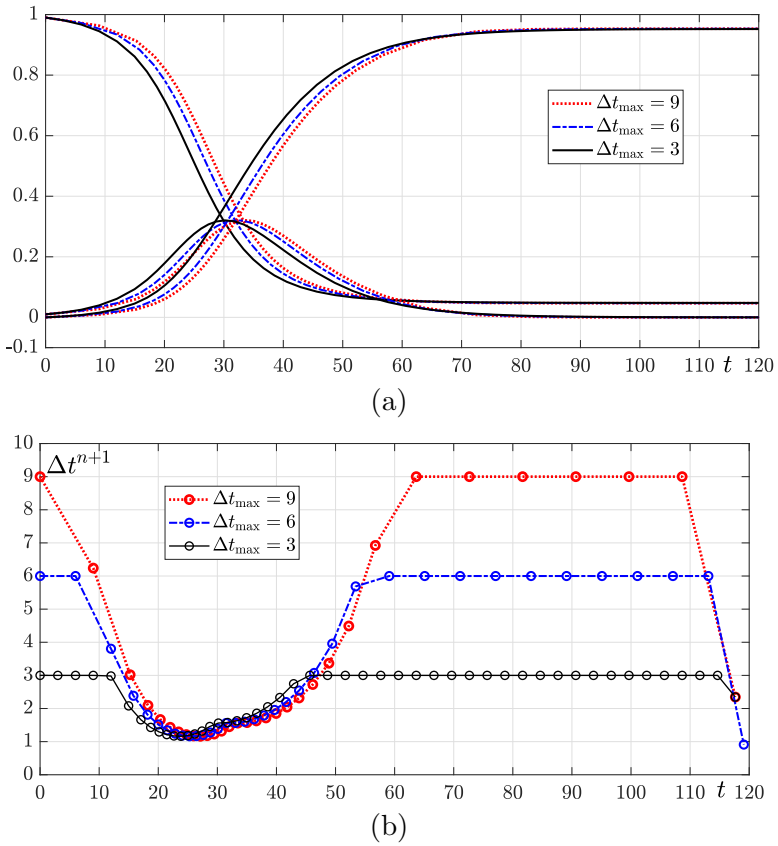

Figure 4: (a) Computational results for $S(t)$, $I(t)$, and $R(t)$ for three different values of the maximum step size of $\Delta t_{\max}$. (b) The adaptive discrete time steps. The parameters used are $\beta = 0.3$, $\gamma = 0.1$, $S_0 = 0.99$, $I_0 = 0.01$, $R_0 = 0$, $T = 120$, and $tol = 0.1$.

finer resolution during rapid transitions, such as near the infection peak, and optimizes step sizes as the system approaches equilibrium. The proposed method is straightforward to implement and eliminates the need for repeated recalculations to satisfy tolerance constraints, making it highly efficient. These advantages make it a promising tool for a wide range of epidemic models, including those with additional compartments or complex dynamics. A limitation of the proposed method lies in its reliance on a first-order scheme. Developing a second-order scheme would be beneficial to improve accuracy, although it poses significant challenges. For future research, the proposed method could be extended to solve partial differential equations, such as the diffusion equation [7] and fractional models [5], to broaden its applicability and demonstrate its effectiveness in solving more complex problems.

Acknowledgements

This work was supported by the National Research Foundation(NRF), Korea, under project BK21 FOUR. I sincerely thank the reviewers for their valuable comments and

constructive suggestions, which have significantly contributed to improving the quality and clarity of this manuscript.

References

[1] I. Cooper, A. Mondal, and C.G. Antonopoulos. A SIR model assumption for the spread of COVID-19 in different communities. *Chaos, Solitons and Fractals*, 139:110057, 2020.

[2] A. Gómez-Corral, F. Palacios-Rodríguez, and M.T. Rodríguez-Bernal. On the exact reproduction number in SIS epidemic models with vertical transmission. *Computational and Applied Mathematics*, 42:291, 2023.

[3] Y. Hwang, S. Kwak, and J. Kim. Long-Time Analysis of a Time-Dependent SUC Epidemic Model for the COVID-19 Pandemic. *Journal of Healthcare Engineering*, 2021:5877217, 2021.

[4] F.Z. Jaouimaa, D. Dempsey, S. Van Osch, S. Kinsella, K. Burke, J. Wyse, and J. Sweeney. An age-structured SEIR model for COVID-19 incidence in Dublin, Ireland with framework for evaluating health intervention cost. *PLOS ONE*, 16(12):e0260632, 2021.

[5] M. Khader. Using Modified Fractional Euler Formula for Solving the Fractional Smoking Model. *European Journal of Pure and Applied Mathematics*, 17(4):2676–2691, 2024.

[6] H. Kim, S. Kwak, M. Mohammed, S. Kang, S. Ham, and J. Kim. An efficient and accurate adaptive time-stepping method for the Landau–Lifshitz equation. *Algorithms*, 18(1):1, 2025.

[7] J. Kim, S. Kwak, H. G. Lee, Y. Hwang, and S. Ham. A maximum principle of the Fourier spectral method for diffusion equations. *Electronic Research Archive*, 31(9):5396–5405, 2023.

[8] S. Kwak, S. Kang, S. Ham, Y. Hwang, G. Lee, and J. Kim. An unconditionally stable difference scheme for the two-dimensional modified Fisher–Kolmogorov–Petrovsky–Piscounov equation. *Journal of Mathematics*, 2023:Article ID 5527728, 2023.

[9] C. Lee, J. Park, S. Kwak, S. Kim, Y. Choi, S. Ham, and J. Kim. An adaptive time-stepping algorithm for the Allen–Cahn equation. *Journal of Function Spaces*, 2022:Article ID 2731593, 2022.

[10] Q. Liu and D. Jiang. Stationary distribution and probability density for a stochastic SEIR-type model of coronavirus (COVID-19) with asymptomatic carriers. *Chaos, Solitons and Fractals*, 169:113256, 2023.

[11] F. Nill. Endemic oscillations for SARS-COV-2 Omicron—A SIRS model analysis. *Chaos, Solitons and Fractals*, 173:113678, 2023.

[12] M. Pájaro, N.M. Fajar, A.A. Alonso, and I. Otero-Muras. Stochastic SIR model predicts the evolution of COVID-19 epidemics from public health and wastewater data in small and medium-sized municipalities: A one year study. *Chaos, Solitons and Fractals*, 164:112671, 2022.

[13] C.M. Pinto, J.A. Tenreiro Machado, and C. Burgos-Simón. Modified SIQR model for

the COVID-19 outbreak in several countries. *Mathematical Methods in the Applied Sciences*, 47(5):3273–3288, 2024.

[14] A.K. Sabherwal, A. Sood, and M.A. Shah. Evaluating mathematical models for predicting the transmission of COVID-19 and its variants towards sustainable health and well-being. *Discover Sustainability*, 5:38, 2024.

[15] S. Sarin, S. Singh, S. Kumar, S. Goyal, B. Gupta, V. Arya, and K. Chui. SEIR-driven semantic integration framework: Internet of Things-enhanced epidemiological surveillance in COVID-19 outbreaks using recurrent neural networks. *IET Cyber-Physical Systems: Theory and Applications*, 9:135–149, 2024.

[16] F.J. Schwarzendahl, J. Grauer, B. Liebchen, and H. Löwen. Mutation induced infection waves in diseases like COVID-19. *Scientific Reports*, 12(1):9641, 2022.

[17] A.A. Thirthar, H. Abboubakar, A. Khan, and T. Abdeljawad. Mathematical modeling of the COVID-19 epidemic with fear impact. *AIMS Mathematics*, 8(3):6447–6465, 2023.

[18] Y. Wang, F. Yuan, Y. Song, H. Rao, L. Xiao, H. Guo, et al. Prediction of cross-border spread of the COVID-19 pandemic: A predictive model for imported cases outside China. *PLOS ONE*, 19(4):e0301420, 2024.